Supplement of Ocean Sci., 22, 1213–1236, 2026
https://doi.org/10.5194/os-22-1213-2026-supplement

Ocean Science Open Access EGU

Supplement of

Sensitivity of marine heatwaves metrics to SST products, focusing on the Tropical Pacific

Carla Chevillard et al.

Correspondence to: Carla Chevillard (carla.chevillard@ifremer.fr, carla.chevillard2@gmail.com)

- **Mean MHW metrics and their anomalies.**

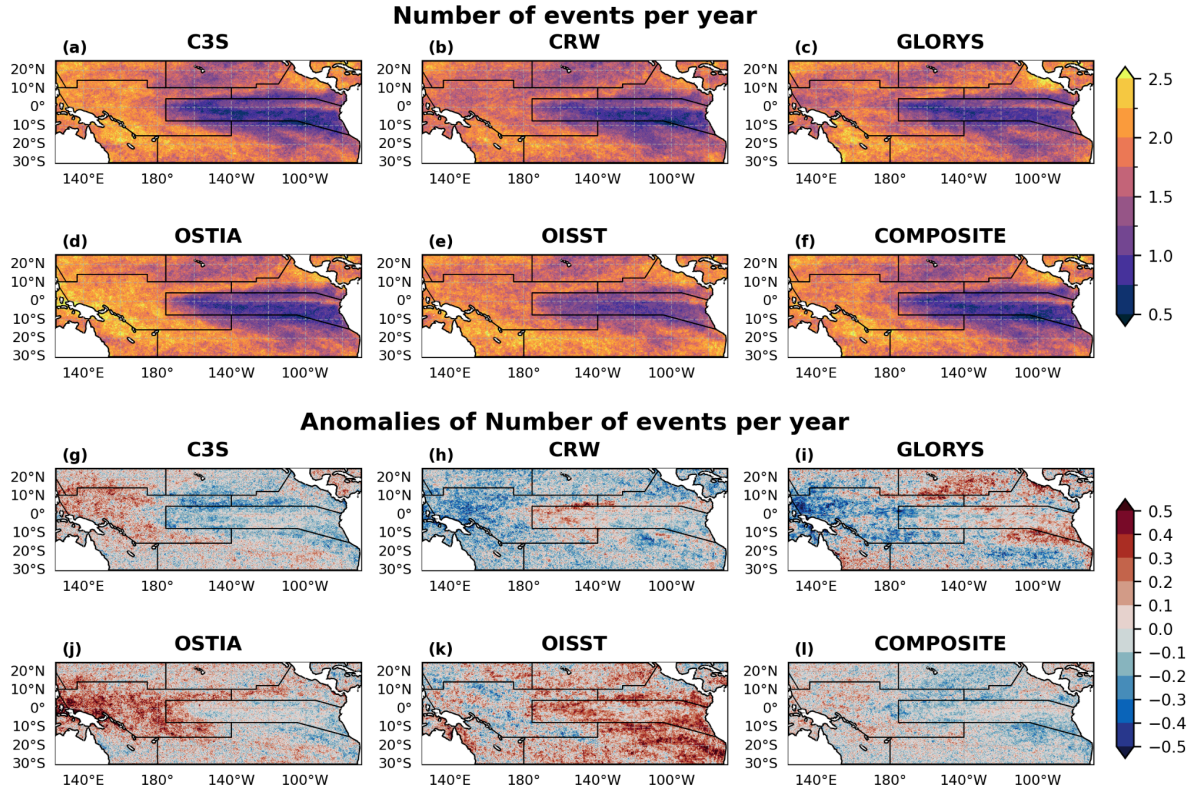

Figure S1: (a-f) Number of MHW events per year over the period 1993-2021 for the six SST products. (g-l) Anomalies of MHW events per year for each product relative to the ensemble mean (section 2.3.1). Black lines indicate regions' limits.

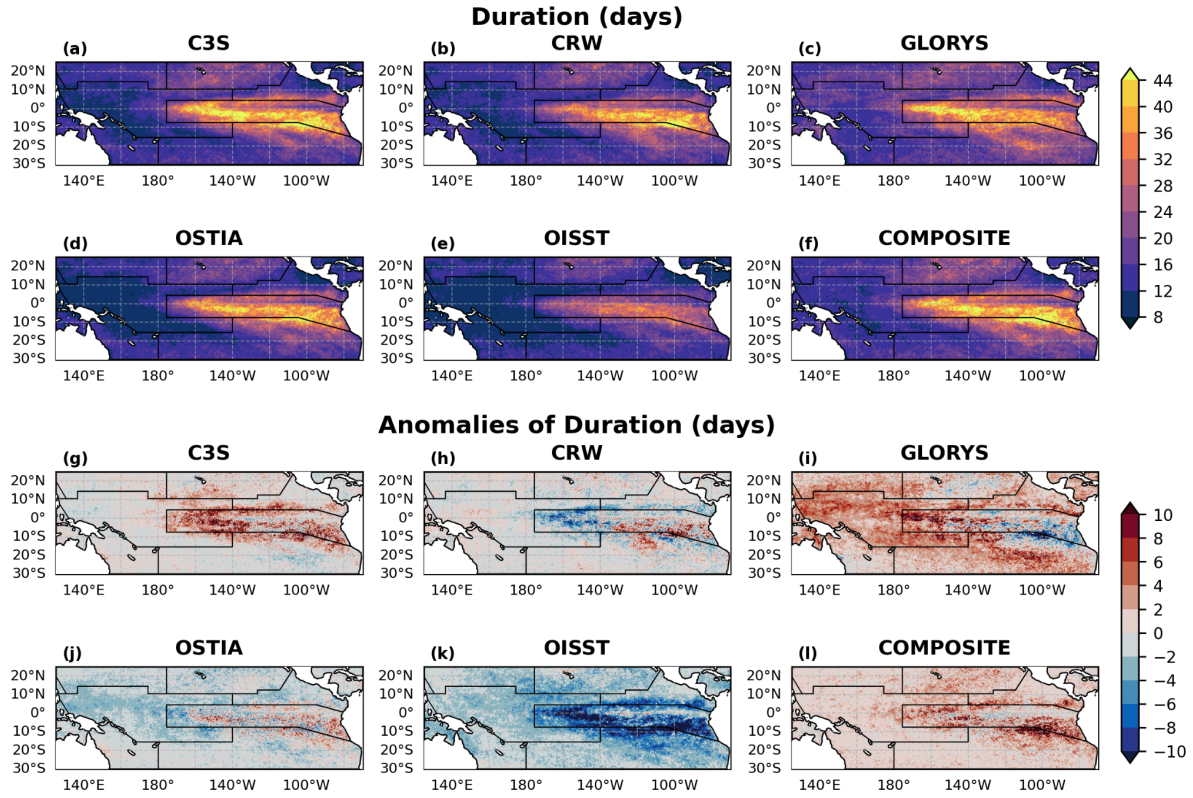

Figure S2: Same as Fig. S1 for the duration metric.

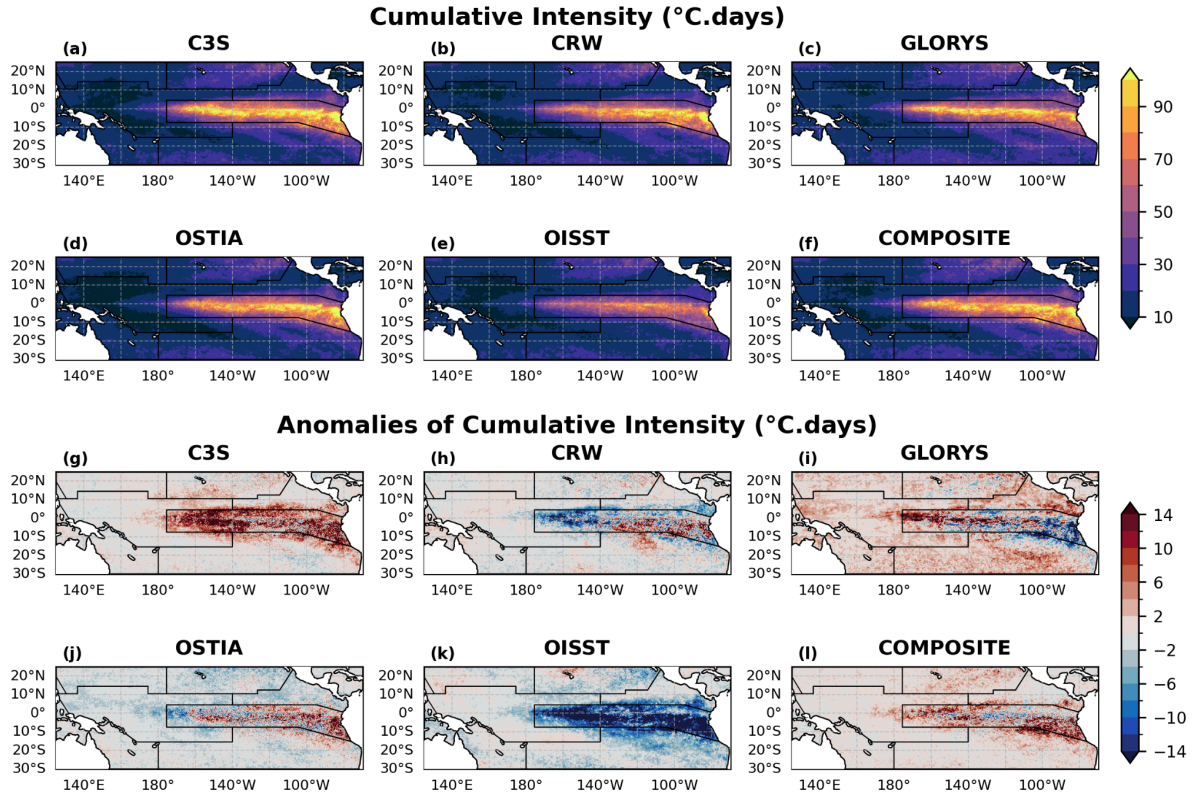

Figure S3: Same as Fig. S1 for the cumulative intensity metric.

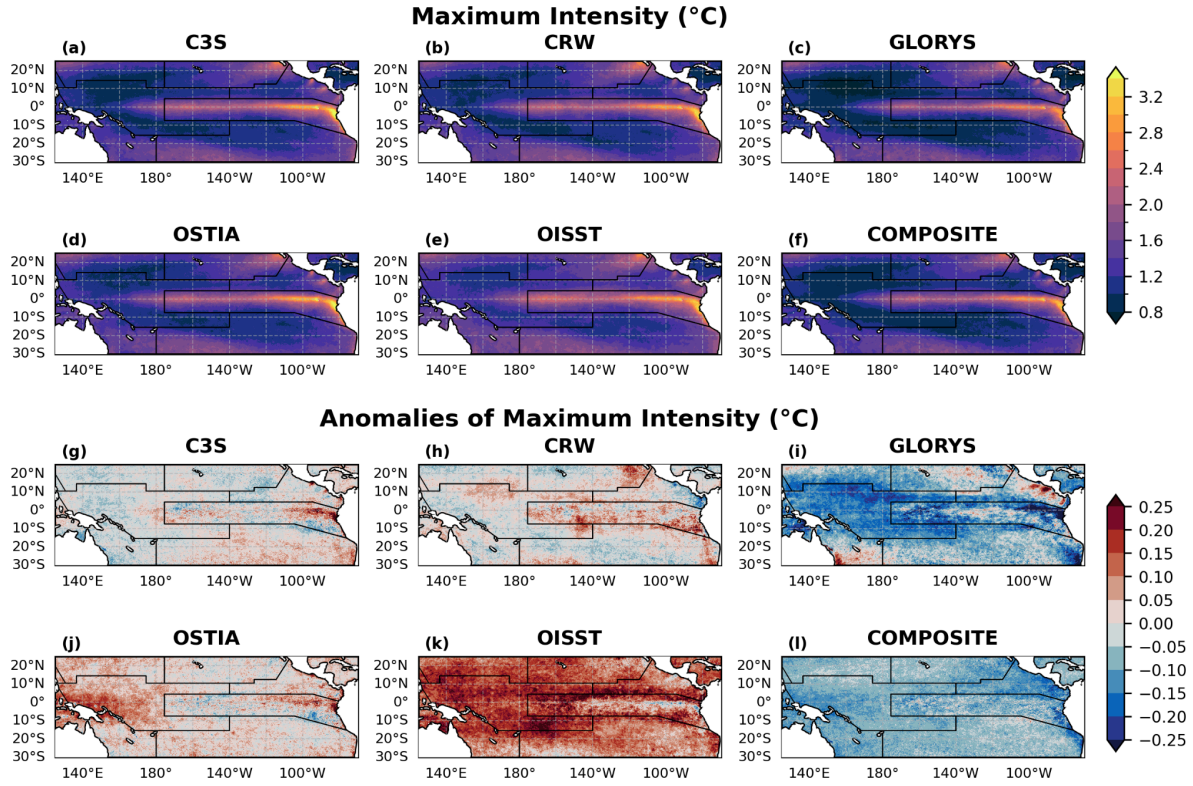

Figure S4: Same as Fig. S1 for the maximum intensity metric.

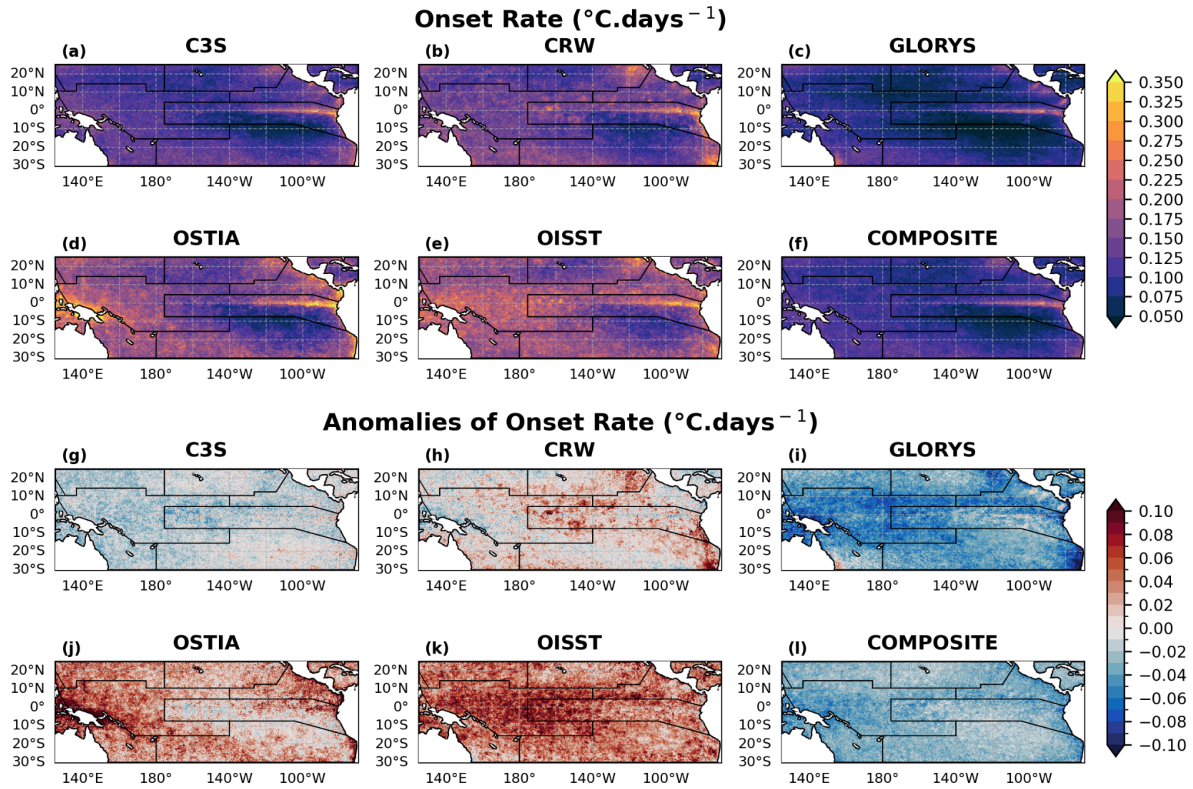

Figure S5: Same as Fig. S1 for the onset rate metric.

Supplementary on Fig. S1-S5

Maps of the total number of events per year for all products (Fig. S1) show the highest differences in the Warm Pool area, with OSTIA reaching more than 2 events per year and CRW ~1 event per year. Anomalies regarding the ensemble mean metric range between +/- 0.5 events per year, the strongest positive anomalies being observed in the Western tropical Pacific for OSTIA and in the eastern tropical Pacific for OISST. The strongest negative anomalies are observed in the Warm Pool area for GLORYS12v1 . For this metric, the COMPOSITE product shows the most neutral anomalies over the whole basin. Contrary to the total MHW days per year, anomalies for this metric significantly vary spatially, and can be either positive or negative in the tropical Pacific for the same product. C3S and OSTIA show positive anomalies on the western part of the tropical Pacific with negative anomalies in the eastern part, while OISST and GLORYS12v1 show the opposite (positive anomalies in the eastern tropical Pacific and negative anomalies in the western part).

Inter-product differences on MHW duration (Fig. S2) can reach more than 20 days in some parts of the tropical Pacific : mean duration is equal to ~25 days for OISST in the PEQD, while it goes up to 50 days for the COMPOSITE. Anomalies for this metric range between -10 and +10 days per year, GLORYS and the COMPOSITE products (OISST) showing the strongest positive (negative) anomalies in the PEQD (area of influence of ENSO). CRW and OSTIA show the most neutral anomalies. Anomalies vary spatially for OSTIA, and CRW, with a tendency to show low negative anomalies over the basin but higher positive anomalies in the central eastern part. The opposite is observed for GLORYS12v1. OISST and the COMPOSITE show spatially uniform anomalies over the tropical Pacific. Same results are observed for the cumulative intensity metric (Fig. S3), which can vary from 60°C.days near the Equator for OISST to more than 100°C.days with GLORYS12v1 or the COMPOSITE in the same zone.

For MHW maximum intensity (Fig. S4), the largest differences are observed in the coastal area of the PEQD, where the maximum intensity reaches its highest values (more than 3°C for all products). There, differences of more than 0.5°C are observed, the highest positive (negative) anomalies being observed for C3S and OSTIA (GLORYS). While anomalies are uniform spatially for OISST (positive anomalies) and the COMPOSITE product (negative anomalies), they vary spatially for the other products. GLORYS12v1 shows negative anomalies in most parts of the basin with hotspots of strong positive anomalies off the Australian and Central American coasts.

The onset rate of MHW shows significant differences as illustrated in Fig. S5. The highest inter-product differences are observed close to the Indonesian Coast, where OSTIA detected onset rates of more than 0.35°C/days while they reached 0.1°C/days with GLORYS12v1. High positive (negative) anomalies are also observed for OISST (COMPOSITE). Over the basin, C3S shows the most neutral anomalies. Anomalies for CRW and C3S vary spatially while they are uniform for the other products.

- **Link with ENSO events.**

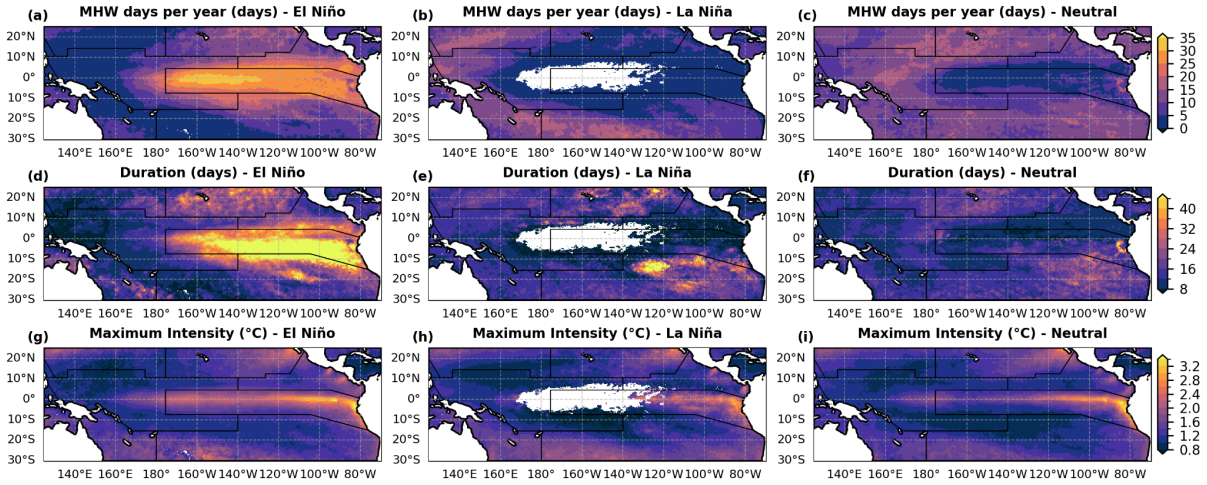

Figure S6: Ensemble mean of MHWs mean statistics for El Niño MHWs (a,d,g), La Niña MHWs (b,e,h) and neutral MHWs (c,f,i).

- **Temporal evolution of ensemble dispersion and spatial correlation.**

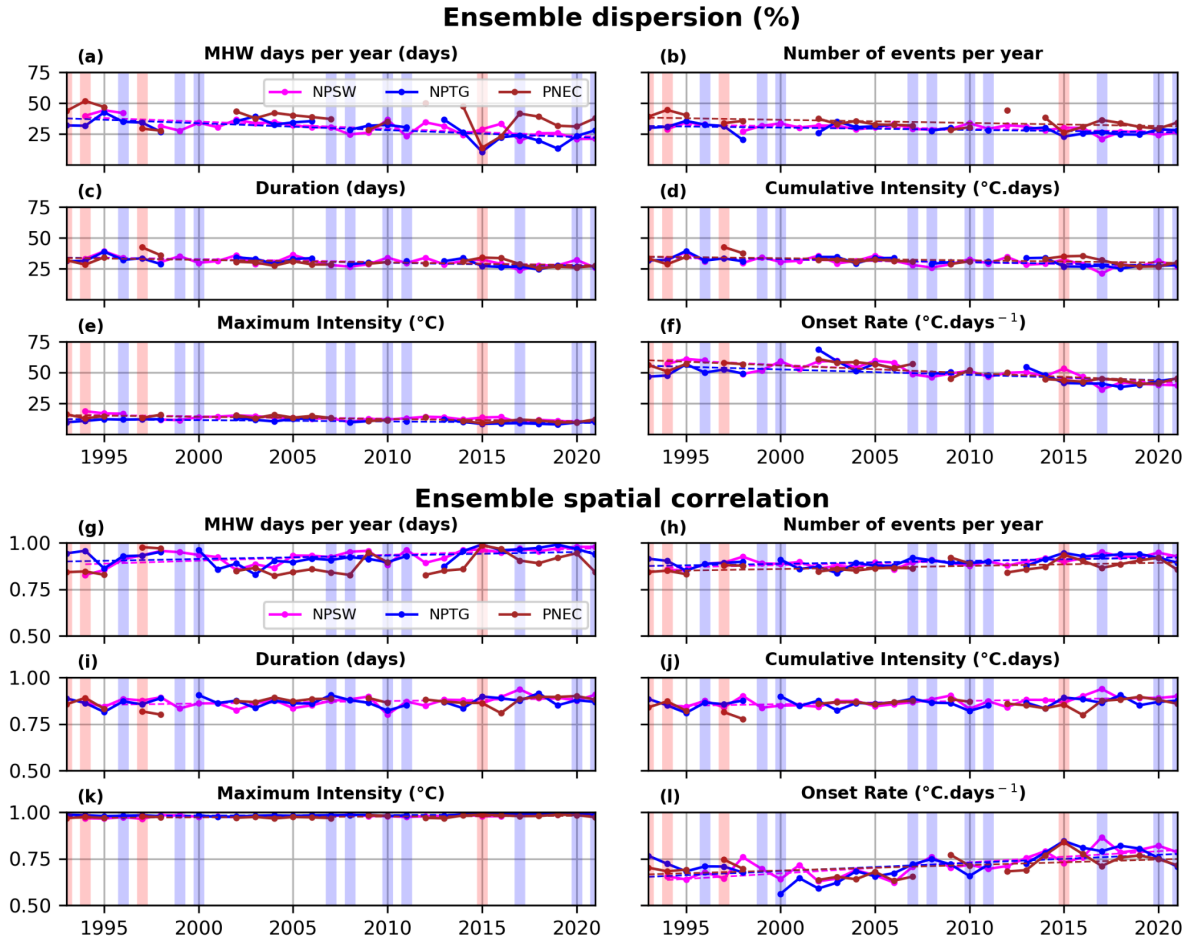

Figure S7: (a-f) Yearly time series of ensemble dispersion (in percentage) for NPSW, NPTG and PNEC. The dashed lines indicate the linear trends, when significant (p_value<0.05). The red and blue backgrounds indicate years of strong El Niño and La Niña, respectively, according to the ONI. (g-l) Same as (a-f) for the ensemble spatial correlation (section 2.2.3). Time series in the PNEC, NPTG and NPSW are represented in Supplementary Fig. S6.

- **Impact of re-gridding.**

The impact of re-gridding on our results was investigated for C3S, CRW and OSTIA, which were all three re-gridded from 0.05° to 0.25°, as well as for GLORYS12v1, which was re-gridded from 0.08° to 0.25°. To investigate the impact of re-gridding, we first analysed simple statistics on SST time series between raw datasets (0.05° and 0.08° for GLORYS12v1) and regridded datasets (0.25°). The main characteristics of SST time series standard deviation - the spatial minimum, maximum, mean and percentile 90 - were computed inside the seven regions studied, for the raw and the regridded datasets. Very little differences were observed between the two datasets for these characteristics, except for the maximum of standard deviation in the NPTG and PNEC. Yet, if the re-gridding induced a slight decrease in the maximum of standard deviation (certainly due to the smoothing of time series when computing the spatial mean of SST within a 0.25°x0.25° pixel), the order of magnitude in the products remained the same (meaning the largest standard deviation maximum or minimum remains the same for both raw and regridded datasets). This analysis suggests that the re-gridding has little impact on our results since we focus on interproducts comparison.

RAW / REGRID	STD MIN	STD MAX	STD MEAN	STD PERC 90
NPSW				
C3S	0.77 / 0.78	2.81 /2.79	1.44 / 1.43	2.13 / 2.13
CRW	0.73 / 0.73	2.80 / 2.78	1.42 / 1.42	2.13 / 2.13
OSTIA	0.74 / 0.75	2.81 / 2.79	1.42 / 1.42	2.13 / 2.13
GLORYS	0.69 / 0.70	2.93 / 2.82	1.41 / 1.41	2.14 / 2.14
NPTG				
C3S	0.79 / 0.78	4.74 / 4.64	1.29 / 1.29	1.71 / 1.71
CRW	0.75 / 0.75	4.46 / 4.35	1.26 / 1.26	1.70 / 1.70
OSTIA	0.76 / 0.76	4.66 / 4.54	1.28 / 1.28	1.71 / 1.71
GLORYS	0.71 / 0.71	4.43 / 4.43	1.30 / 1.30	1.73 / 7.73
WARM				
C3S	0.41 / 0.41	1.21 / 1.20	0.74 / 0.73	0.94 / 0.93
CRW	0.45 / 0.45	1.16 / 1.16	0.71 / 0.71	0.90 / 0.90
OSTIA	0.33 / 0.36	1.15 / 1.15	0.72 / 0.71	0.91 / 0.91
GLORYS	0.88 / 0.88	1.25 / 1.19	0.67 / 0.67	0.88 / 0.88
PNEC				
C3S	0.68 / 0.69	4.20 / 4.04	1.06 / 0.06	1.43 / 1.45
CRW	0.62 / 0.62	3.92 / 3.85	1.02 / 1.02	1.33 / 1.33
OSTIA	0.51 / 0.51	4.07/3.97	1.03 / 1.03	1.38 / 1.39
GLORYS	0.67 / 0.68	4.16 / 3.96	1.04 / 1.04	1.37 / 1.38

PEQD				
C3S	0.56 / 0.56	3.10 / 3.10	1.56 / 1.56	2.63 / 2.63
CRW	0.56 / 0.56	3.10 / 3.10	1.53 / 1.53	2.55 / 2.55
OSTIA	0.53 / 0.53	3.07 / 3.06	1.53 / 1.53	2.56 / 2.56
GLORYS	0.51 / 0.51	3.06 / 2.94	1.48 / 1.48	2.47 / 2.47
SPSG				
C3S	0.77 / 0.76	3.16 / 3.15	1.56 / 1.56	2.13 / 2.12
CRW	0.77 / 0.77	3.05 / 3.05	1.54 / 1.54	2.12 / 2.12
OSTIA	0.71 / 0.73	3.08 / 3.07	1.54 / 1.54	2.11 / 2.11
GLORYS	0.75 / 0.75	2.94 / 2.93	1.53 / 1.53	2.10 / 2.10
ARC				
C3S	0.58 / 0.59	3.31 / 3.30	1.60 / 1.60	1.92 / 1.92
CRW	0.57 / 0.57	3.27 / 3.27	1.58 / 1.58	1.93 / 1.94
OSTIA	0.44 / 0.45	3.27 / 3.23	1.58 / 1.57	1.93 / 1.93
GLORYS	0.59 / 0.60	3.44 / 3.41	1.62 / 1.62	1.97 / 1.97

Table S1 : spatial minimum, maximum, mean and 90th percentile of the standard deviation of SST time series inside each region of study for the raw (0.05° for C3S, CRW and OSTIA ; 0.08° for GLORYS) and regridded (0.25°) datasets of C3S, CRW, OSTIA and GLORYS.

Then, MHW statistics were computed from the raw datasets at 0.05° resolution (0.08° for GLORYS12v1) and compared to the results of the 0.25° dataset for C3S, CRW, OSTIA and GLORYS12v1, inside two small areas of study : one in the ARC subregion corresponding to the area around New Caledonia (155E - 175E ; 14S - 27S, shown in Fig. S8) and one in the Warm Pool subregion (150E-170E ; 0-10N). We focused on small areas as computing MHW statistics at 0.05° or 0.08° resolution over the tropical Pacific was very costly in terms of computation. Since results between the two areas of study were similar, only the study case of New Caledonia is presented here.

As one pixel of the regridded datasets corresponds to 25 pixels of the raw datasets, we associated each pixel of the regridded dataset to its 25 pixels in the raw grid and computed the mean and standard deviation of MHW statistics inside these 25 pixels. Fig. S8 illustrates the method for the metric duration (not shown for the other metrics): panels a to d represent the MHW detection performed over the four raw datasets in the area of New Caledonia; panels e to f represent the mean of MHW statistics of the 0.05° grid inside the 0.25°grid; and panels i to l represent the MHW detection performed over the four re-gridded SST datasets at 0.25° used in the study. Then, to quantify the impact of re-gridding, we computed the re-gridding error as well as the information lost in the re-gridding process.

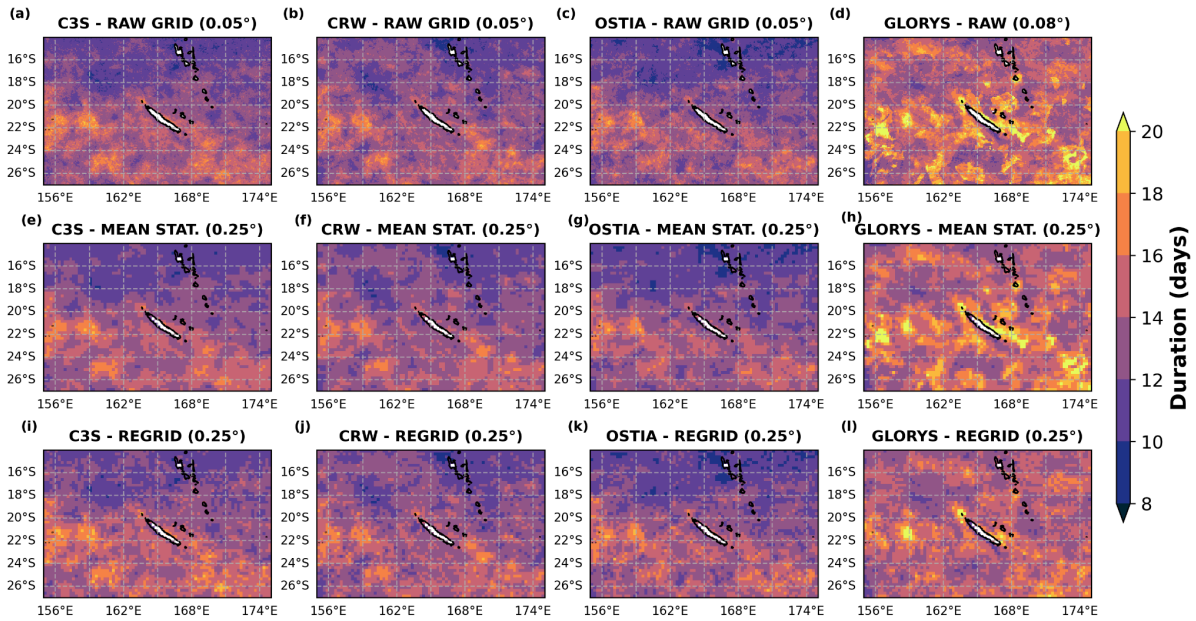

Figure S8: (a-d) Mean duration of MHWs for detection performed over 1993-2021 for C3S (a), CRW (b) and OSTIA (c) at 0.05° resolution, and for GLORYS (d) at 0.08° resolution. (e-h) Mean of MHW duration values of the detection performed at 0.05° (0.08° for GLORYS) inside the 0.25° grid for C3S (e), CRW (f), OSTIA (g) and GLORYS (h) (i-l) Mean duration of MHWs for detection performed over 1993-2021 for C3S (i), CRW (j), OSTIA (k) and GLORYS (l) at 0.25° resolution.

The re-gridding error was defined as the difference between MHW statistics computed from the regridded datasets (Fig. S8i-l) and the mean of the 25 MHW statistics of the raw grid inside the 0.25° grid (Fig. S8 e-h). Maps of the re-gridding error for all metrics in the area of New Caledonia (not shown) highlighted that the maximum intensity and onset rate show lower values in the regridded datasets compared to the raw dataset (negative values over the whole area, not shown), and the MHW days per year shows higher values (especially for C3S, not shown) in the regridded dataset. This result is in line with the fact that the re-gridding induces a smoothing of the SST signal and thus will detect more MHW days and lower maximum intensities and onset rates. Then, the re-gridding error was expressed in percentage by dividing it by the mean value of the statistics of the 0.05° grid inside the 0.25° grid, to give the re-gridding error in percentage. The spatial mean over the area of New Caledonia of the re-gridding error in percentage was computed for each dataset and variable, and is illustrated in Fig. S9a.

In the same way we computed the mean of the 25 values of MHW statistics of the raw grid inside the 0.25° grid to define the re-gridding error, we computed the standard deviation of the 25 values of MHW statistics of the raw grid inside the 0.25° grid. Then, by dividing it by the associated mean value of the statistics of the 0.05° grid inside the 0.25° grid, we defined the information loss during the re-gridding process. This quantity is illustrated in Fig. S9b for all metrics (spatial mean over the area of New Caledonia).

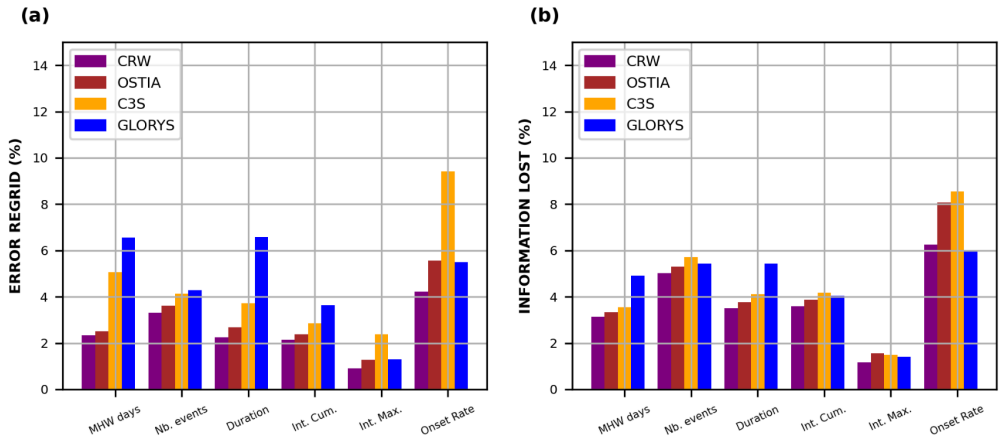

Figure S9: spatial mean over the area of New Caledonia of the re-gridding error expressed in percentage (a) and information lost in the re-gridding process (b) as defined in the text.

For C3S, CRW and OSTIA, the re-gridding error is lower than 4% for all metrics except the onset rate for which it ranges between 4 and almost 10% (Fig. S9a). GLORYS12v1 appears to be more impacted than the other products by the re-gridding, except for the onset rate and maximum intensity metrics for which C3S shows the largest regridding errors (Fig. S9a). Similar observations can be made for the percentage of information lost (Fig. S9b), which is lower than 5/6% for all metrics and products except for the onset rate for which it ranges between 6 and 8/9%. If Fig. S9 shows that the re-gridding process has an influence on MHW statistics, these values of re-gridding error and information loss are rather low and suggest that the re-gridding process has little impact on our results. Yet, the higher re-gridding error and information loss for the onset rate, as well as the difference of impact between products might play a role in the higher inter-products dispersion observed for this metric. If the impact of re-gridding is negligible for most MHW metrics, it might therefore not be the case for the onset rate. Let's also note that for all metrics, the re-gridding error is rather similar between C3S and OSTIA while it is quite different from C3S and GLORYS, for which it is higher for all metrics. The higher impact on C3S and GLORYS might be due to a higher spatial variability at finer scales for these products, thereby generating more impacts of the re-gridding.